

	SAKARYA ÜNİVERSİTESİ FEN BİLİMLERİ ENSTİTÜSÜ DERGİSİ <i>SAKARYA UNIVERSITY JOURNAL OF SCIENCE</i>		
	e-ISSN: 2147-835X Dergi sayfası: http://dergipark.gov.tr/saufenbilder		
	<u>Geliş/Received</u> 05.12.2016 <u>Kabul/Accepted</u> 26.05.2017	<u>Doi</u> 10.16984/saufenbilder.270251	

Stability analysis of the automatic voltage regulation system with PI controller

Mahmut Temel Özdemir^{*1}, Vedat Çelik²

ABSTRACT

The system voltage is one of the most important parameters, which determines the power quality. The stability of the system voltage is critical for the power system. This paper investigates the stability analysis of the automatic voltage regulation system controlled by a PI controller related to the controller gains. For this purpose, a graphical-based technique called as the stability boundary locus method is proposed in the paper to obtain the stable parameters space of PI controller gains. Stability of closed region computed on parameters space determines from roots of characteristic equation of automatic voltage regulation system. The time-domain simulations are performed in Matlab/Simulink environment to validate the theoretical results.

Keywords: Automatic voltage regulation, stability boundary locus, stable parameters space, electric power system, PI controller

PI Kontrolörlü otomatik gerilim regülasyon sisteminin kararlılık analizi

ÖZ

Elektrik güç sistemlerinde güç kalitesine etki eden en önemli parametre sistem gerilimidir. Sistem geriliminin kararlılığı güç sistemi açısından çok kritik öneme sahiptir. Bu çalışma, otomatik gerilim regülasyon (OGR) sisteminde PI kazançlarının değerlerine bağlı olarak sistem kararlılığını analiz etmiştir. Bu amaçla, kararlı PI parametre uzayını elde etmek için grafik tabanlı olan kararlılık sınır eğrisi metodu önerilmiştir. OGR sisteminin karakteristik denkleminin köklerine göre kararlılık kapalı bölgesi hesaplanmıştır. Teorik olarak elde edilen bu bölge, Matlab/Simulink ortamında gerçekleştirilen zaman domain benzetimleri ile doğrulanmıştır.

Anahtar Kelimeler: Otomatik gerilim regülasyonu, kararlı sınır eğrisi, kararlı parametre uzayı, elektrik güç sistemi, PI kontrolör

¹ Fırat University, Faculty of Engineering, Department of Electrical and Electronics Engineering, 23119, Elazığ, Turkey (e-mail: mto@firat.edu.tr)

² Fırat University, Faculty of Engineering, Department of Electrical and Electronics Engineering, 23119, Elazığ, Turkey (e-mail: celik@firat.edu.tr)

1. INTRODUCTION

The system that provides electrical energy flow from electricity production centers to consumption centers is called an interconnected system. This energy flow should be continuously provided on demand for system stability [1]–[3]. The active and/or reactive power change occurring in demand shows itself in two different ways in the electricity production center. The first one is the case resulted in the change of frequency of the system, that is, rotation speed of the generator. Load frequency control systems are used to hold at the desired frequency [4]–[6]. The second one is the change occurring in the terminal voltage of the generator due to the change especially in reactive power. Generator excitation control or automatic voltage regulator (AVR) systems are used to keep the terminal voltage at nominal values [7]–[9]. When these two parameters (frequency and voltage) can not be maintained at the desired values, the power system can black out. This condition is one of the most tragic scenarios for a power system.

Voltage sag occurs as a result of voltage instability caused by voltage drop in most of systems [4], [10]. One of the most important issues needed to be overcome in power systems is voltage sags and drops [10]. Transformers whose electrical connections are changed via mechanical or static switches, saturated reactor regulators, phase controlled regulators, ferro resonance transformers and motorized variac can be used to handle this problem as first solution [4]. The second solution uses AVR that keeps the generator voltage at the desired value. The primary goal of AVR is ensuring that output voltage or reactive power is kept at absolute value by controlling the excitation current in case of nominal, small and slow changes occurring in the reactive loads [1], [3], [11]. AVR is the control mechanism that detects variations in the output voltage of the generator and provides a controlling excitation current. If the response of regulator is slow; that means it has a dead band and is insensitive to changes. This is not a desired situation. Therefore AVR is a critical component of the power systems. Thus, it should detect even small variations in the output voltage of the system and generate a feedback signal proportional to this value by its control system [1], [3], [11]. Even though AVRs support the power system to maintain its synchronism by increasing the synchronizer torque value with their high

operating speeds, they cause deterioration of dynamic stability of the power system due to their reducing effect of damping torque. Control system called power system stabilizer for producing assistive control signals is added to the excitation system to eliminate the negative effect of AVRs on dynamic stability of power systems [12], [13]. At this point, the stability analysis of power system with AVRs is also an important issue.

The response speed of AVRs is critical for stability [1], [13], [14]. Because, AVRs have significant effects on transient events that occur in electrical systems [14]–[16]. For this reason, PID type controllers widely used in the industry due to their simple structure [17] are used in power systems. P controller reduces the steady-state error to a certain extent with the help of proportional gain. On the other hand, it can cause instability or high-frequency oscillations in case of increasing the proportional gain to reduce the steady-state error [17]–[19]. Therefore, integral structure is also added to eliminate steady-state error. Thus, PI controllers are the most widely used PID type controllers.

The primary objective is to run the system in a stable parameters space in all control systems. For this purpose, many studies have been conducted to compute stable parameters space [8], [19]–[23]. In those studies, systems using PI and PID controllers as the controller with [19]–[21], [24] and without [22], [23] time-delay has been investigated.

In this study, it has been aimed to compute the stable parameter space of controller gains when AVR system is controlled by a *PI* controller. To obtain the stable parameter space, stability boundary locus method which is a frequency based graphical method given in [25] will be used. The obtained results will be verified by time domain simulations. After the introduction, in the second section the structure of AVR systems with *PI* controller and stability boundary locus of this system will be determined. In the third section, stability boundary locus of the system in K_p – K_i space will be computed by utilizing the analytical results which are obtained, and time-domain simulations will be presented. In the last section of this study, the results will be discussed.

2. MATERIAL AND METHOD

Voltage regulators are the center of excitation systems in terms of many aspects [1], [11], [18].

AVR enables regulating effect by detecting changes in the output voltage. Previously, this regulation was manually performed in the voltage regulation systems. In these systems, the terminal voltage of generator used to be changed by a rheostat on the exciting current until the desired output voltage is reached.

2.1. The automatic voltage regulation systems with PI controller

In Figure 1, the schematic diagram of an AVR system is presented [11].

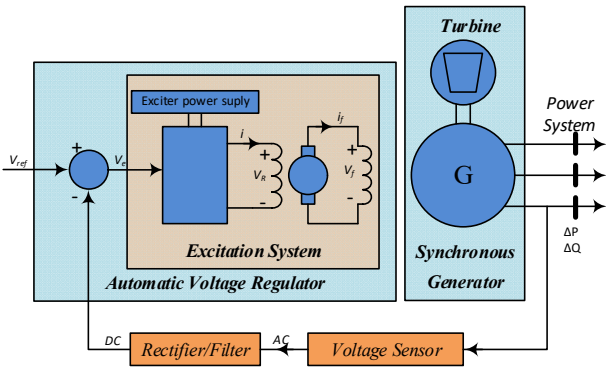


Figure 1. Schematic diagram of AVR of a synchronous generator

Considering Figure 1, any change in the output voltage of the generator will change the terminal voltage. The voltage value measured by a voltage sensor is transmitted to AVR. Then AVR alters the terminal voltage of excitation system to keep the terminal voltage of generator at the desired value. The field current of generator changes by this way. This condition also changes the generated EMF. The power generation of the generator is adjusted to a new equilibrium point and the terminal voltage is maintained at the desired value[11]. Block diagram of AVR system whose schematic diagram is presented in Figure 1 is given in Figure 2.

AVR given in Figure 2 is the system that detects the output voltage of the generator and provides the regulating impact by controlling the excitation system to the desired value. In this block diagram, each subsystem is presented as below:

Amplifier Model

Excitation system may be an amplifier which can be a magnetic amplifier, a rotating amplifier or a modern electronic amplifier. The amplifier is defined by a transfer function including K_a gain and τ_a time constant [1], [11], [7], [13], [26].

$$G_a(s) = \frac{K_a}{1 + \tau_a s}$$

A typical value of K_a is between 10 and 500 and the typical value of τ_e in the range of 0.02-0.1 seconds [1], [11], [7], [13], [26].

Excitation Model

These are DC-based excitation, AC-based excitation and static based excitation [27]–[29]. In modern excitation systems, there are the linear models that take time constant into account but ignore saturation or other non-linear structures. The relationship between output voltage and the terminal voltage of the excitation system is a function non-linear with saturation effect in the magnetic circuit [27]–[29]. In its simplest form, the transfer function of modern excitation is defined with τ_e time constant and K_e gain is obtained as below.

$$G_e(s) = \frac{K_e}{1 + \tau_e s}$$

A typical value of K_e is between 1 and 10 and the typical value of τ_e in the range of 0.4-1.0 seconds [1], [11], [7], [13], [26]

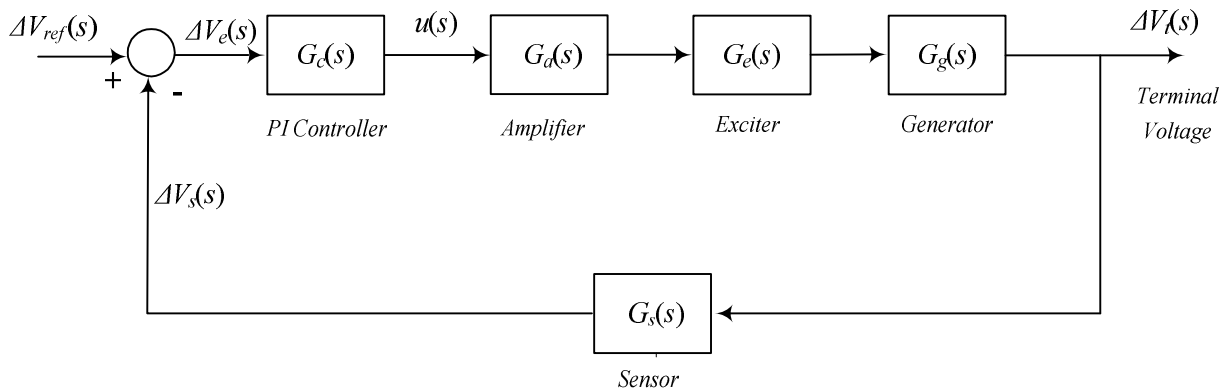


Figure 2. Block diagram of AVR system

Generator Model

Electromagnetic force generated by the synchronous machines is a function of machine magnetization curve. Terminal voltage depends on the generator load. In the linearized model, the transfer function is defined with K_g gain and τ_g time constant.

$$G_g(s) = \frac{K_g}{1 + \tau_g s}$$

These constants change depending on fully loaded or unloaded system. K_g gain varies between 0.7 and 1 and τ_g may vary within the range of 1.0 to 2.0 seconds [1], [11], [7], [13], [26]

Sensor Model

The sensor converts the terminal voltage of AC generator into the DC form so that error signal can be obtained.

$$G_s(s) = \frac{K_s}{1 + \tau_s s}$$

It can be modeled by simple first-degree transfer function of a sensor. τ_s is very small and varies between 0.01 and 0.06 seconds [1], [11], [7], [13], [26]

PI Controller Model

The transfer function of the PI controller is:

$$G_c(s) = K_p + \frac{K_i}{s}$$

where K_p and K_i are proportional and integral gains respectively.

By using the defined subsystems as above, transfer function of the system given in Figure 2 is obtained as follows:

$$aa = K_a K_e K_g (K_p s + K_i)(1 + \tau_s s)$$

$$bb = s(1 + \tau_a s)(1 + \tau_e s)(1 + \tau_g s)(1 + \tau_s s) + K_a K_e K_g K_s (K_p s + K_i)$$

$$\frac{V_t(s)}{V_{ref}(s)} = \frac{aa}{bb} = \frac{\Delta_N(s)}{\Delta_D(s)} \quad (1)$$

Where numerator polynomial of the transfer function is as below:

$$\Delta_N(s) = q_2 K_p s^2 + q_1 (K_p + \tau_s K_i) s + q_0 K_i = 0 \quad (2)$$

where,

$$q_2 = \tau_s K_a K_e K_g$$

$$q_1 = q_0 = K_a K_e K_g$$

The characteristic equation of the system shown in Figure 2 is obtained as follows:

$$\Delta_D(s, K_p, K_i) = p_5 s^5 + p_4 s^4 + p_3 s^3 + p_2 s^2 + (1 + p_1 K_p) s + p_0 K_i = 0 \quad (3)$$

where,

$$p_5 = \tau_a \tau_e \tau_g \tau_s$$

$$p_4 = \tau_a \tau_e \tau_g + \tau_a \tau_e \tau_s + \tau_a \tau_g \tau_s + \tau_e \tau_g \tau_s$$

$$p_3 = \tau_a \tau_e + \tau_a \tau_g + \tau_e \tau_g + \tau_a \tau_s + \tau_e \tau_s + \tau_g \tau_s$$

$$p_2 = \tau_a + \tau_e + \tau_g + \tau_s$$

$$p_1 = p_0 = K_a K_e K_g K_s$$

Since the roots of characteristic equation of the system are also poles of the system, stability analysis of the system will be performed by utilizing the characteristic equation obtained by the Eq. (3). There are three boundaries according to the characteristic equation. They are real root boundary (RRB), complex root boundary (CRB) and infinite root boundary (IRB) [29].

$$\text{RRB: } \Delta_{D,0}(0, K_p, K_i) = 0$$

$$\text{CRB: } \Delta_{D,\omega}(\pm j\omega, K_p, K_i) = 0$$

$$\text{IRB: } \Delta_{D,\infty}(\infty, K_p, K_i) = 0$$

For stability analysis of the system, RRB is $K_i=0$ and its CRB is $\ell(\omega, K_p, K_i)$, however, because IRB does not depend on K_p, K_i controller parameters, there is no IRB on K_p-K_i plane.

2.2. Argins The stability boundary locus analysis of AVR systems with PI controller

The system will have poles on only the axis of $j\omega$ with K_p and K_i values that will make characteristic equation equal to zero for $s=j\omega$. This case corresponds to the critical stability of the system. It should be made real and imaginary parts of the characteristic equation equal to zero separately to compute gains of PI controller from the equation.

$$\text{Re}[\Delta_D(j\omega)] = p_4 \omega^4 - p_2 \omega^2 + p_0 K_i = 0$$

$$\text{Im}[\Delta_D(j\omega)] = p_5 \omega^5 - p_3 \omega^3 + (1 + p_1 K_p) \omega = 0 \quad (4)$$

Gain values of PI controller can be obtained as below:

$$K_i = \frac{p_2\omega^2 - p_4\omega^4}{p_0} \tag{5}$$

$$K_p = \frac{p_3\omega^2 - p_5\omega^4 - 1}{p_1} \tag{6}$$

Stability boundary locus of the system can be achieved on the K_p-K_i plane for AVR system in the range of $\omega=(0,\infty)$. The change obtained is the parameters that make the system critically stable. The roots of Eq. (3), which are poles of the system, can be determined whether inside of closed region obtained on K_p-K_i plane is stable.

3. RESULTS AND DISCUSSION

In this section, stability boundary locus of AVR system provided with the characteristic equation in the previous section will be obtained, and the region computed on the K_p-K_i plane will be tested. Then, the obtained results will be verified by time domain simulations.

3.1. Computation stability region of AVR systems with PI controller

Stability boundary locus of the system is determined by using Eq. (5) and (6) given in Figure 3 for system parameter values ($K_a=10, K_e=1, K_g=1, K_s=1; \tau_a=0.1 s, \tau_e=0.4 s, \tau_g=1 s, \tau_s=0.01 s$) used in [7].

Considering the stability boundary locus obtained on K_p-K_i plane, the closed region is stable as it will be seen the analysis of the system according to the roots of the characteristic Eq. (3).

One of the boundaries of the stable region is *RRB* which is the line of $K_i=0$. This condition means that the system has only proportional controller K_p and *RRB* line is the border of the instability. The other boundary is *CRB* for the system. This change is obtained from Eq. (5) and (6) by changing ω . This means that the system has a complex conjugate pole on the $j\omega$ axis and is critically stable.

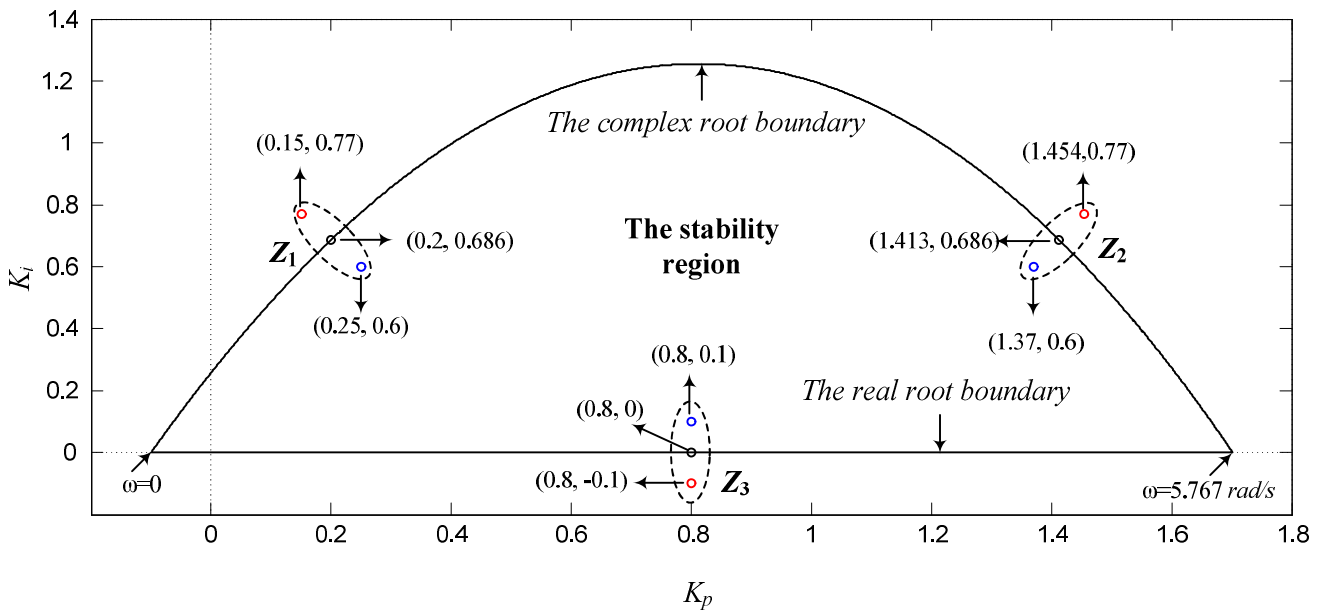


Figure 3. The stability boundary locus of AVR system

Table 1. Poles of the system for PI controller gains pair given Z_1, Z_2 and Z_3

	Gains of PI		Poles of the System				
	K_p	K_i	s_1	s_2	s_3	s_4	s_5
Z_1	0.15	0.77	-99.99	-10.28	-3.55	0.16-j2.28	0.16-j2.28
	0.2	0.686	-99.99	-10.49	-3.01	-j2.32	j2.32
	0.25	0.6	-99.99	-10.68	-2.42	-0.19-j2.39	0.19+j2.39
Z_2	1.45	0.77	-99.95	-13.11	-0.51	0.04-j5.32	0.04+j5.32
	1.413	0.686	-99.95	-13.06	-0.47	-j5.27	-j5.27
	1.37	0.6	-99.96	-13.01	-0.42	-0.05-j5.21	-0.05-j5.21
Z_3	0.8	0.1	-99.97	-12.1	-0.11	-0.65-j4.22	-0.65-j4.22
	0.8	0	-99.97	-12.12	-0.69-j4.25	-0.69-j4.25	---
	0.8	-0.1	-99.97	-12.14	0.1	-0.74-j4.28	-0.74-j4.28

K_p - K_i parameters selected outside of the closed region will destabilize the system. K_p - K_i parameters chosen in the closed region will stabilize the system according to the analysis of the poles of system. The poles of the system for K_p - K_i parameters given in Z_1 , Z_2 and Z_3 have been obtained in Table 1.

The characteristic equation of the system for K_p - K_i parameters pair (0.25, 0.6), which is inside of closed region given in Z_1 , has been obtained as follow:

$$\Delta(s) = 4 \cdot 10^{-4} s^5 + 0.0454 s^4 + 0.555 s^3 + 1.51 s^2 + 3.5 s + 6 = 0$$

In this case the poles of the system are $s_1 = -99.99$, $s_2 = -10.68$, $s_3 = -2.42$ and $s_{4,5} = -0.19 \pm j2.39$. As it is seen, the system has no poles in right half s -plane. Hence, the system is stable for these parameter pairs. Because dominant poles of the system are s_4 and s_5 that are complex conjugate, there will be a damped oscillation in the system. On the other hand, characteristic equation of the system for K_p - K_i parameter pair (0.15, 0.77), which is outside of the closed region given in Z_1 , has been obtained as follows:

$$\Delta(s) = 4 \cdot 10^{-4} s^5 + 0.0454 s^4 + 0.555 s^3 + 1.51 s^2 + 2.5 s + 7.7 = 0$$

Therefore the system poles have been obtained as $s_1 = -99.99$, $s_2 = -10.28$, $s_3 = -3.55$ and $s_{4,5} = 0.16 \pm j2.28$. Note that the system has two complex conjugate poles in right half s -plane and is unstable.

Finally, characteristic equation of the system for K_p - K_i parameter pair (0.2, 0.686), which is on CRB given in Z_1 , has been obtained as follows:

$$\Delta(s) = 4 \cdot 10^{-4} s^5 + 0.0454 s^4 + 0.555 s^3 + 1.51 s^2 + 3 s + 6.86 = 0$$

Poles of this characteristic equation are $s_1 = -99.99$, $s_2 = -10.49$, $s_3 = -3.01$ and $s_{4,5} = \pm j2.32$. According to the poles, the system is critically stable and value of the frequency in this point on K_p - K_i plane is $\omega = 2.32 \text{ rad/s}$. This value is also the frequency of the undamped oscillation occurred in the system for this controller parameters pair.

The similar results are obtained for Z_2 and Z_3 and Table 1 indicates this condition. Because the system for controller gains marked in bold in Table 1 has one pole and one zero at the origin, these two effects will neutralize each other. Therefore, the number of poles of the system will be reduced to

four poles. Considering the poles of the system, it has one real unstable pole and two dominant complex conjugate poles in left half s -plane. Hence, while a damped oscillation is expected in the transient response of the system, output of the system in the steady state will exponentially increase.

3.2. Time domain simulation results

In this section, simulation results for K_p - K_i parameter pairs given in Figure 3 will be presented. Time responses of the system are obtained in Figure 4, Figure 5 and Figure 6 for K_p - K_i parameters in Z_1 , Z_2 and Z_3 respectively.

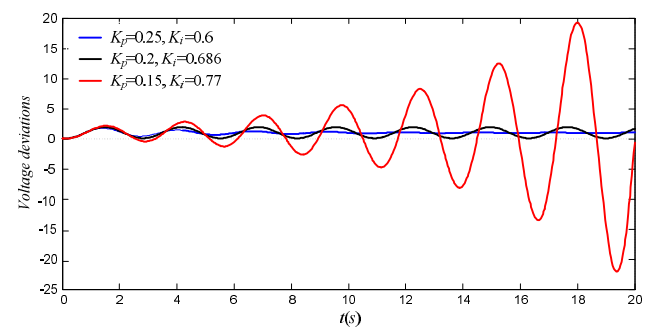


Figure 4. Time responses of the system for parameters in Z_1

As it can be seen in Figure 4 and 5, the response of the system for parameters chosen from stable region illustrates a stable behavior with blue. The response of the system for parameters chosen on stability boundary locus is critically stable with black, and also the response of the system for parameters chosen outside of the stable region is unstable with red. Considering Figure 3, since the frequency value corresponding to parameters on the stability boundary locus in Z_2 is greater than those in Z_1 , frequency of damped oscillations in Z_2 are greater than oscillations in Z_1 as shown in Figure 4 and 5 with responses of the critically stable system in Z_1 and Z_2 .

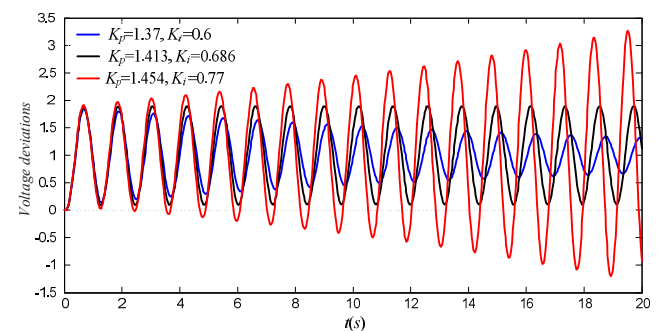


Figure 5. Time responses of the system for parameters in Z_2

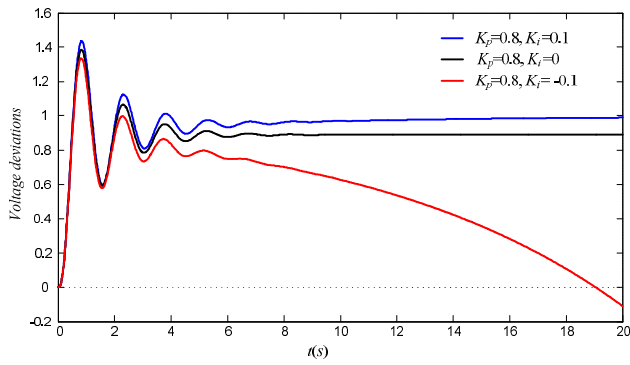


Figure 6. Time responses of the system for parameters in Z_3

As expected, the system is exponentially unstable for the controller gains outside of stability boundary locus for Z_3 . On the other hand, the system is stable for the controller gains inside of stability boundary locus or on it.

4. CONCLUSION

While controlling power systems, it is intended to improve their performances. In this article, however, since it is important to keep the stability for security and efficiency of the system; it has been aimed to determine stable parameter space of PI controller when an AVR system is controlled by a PI controller. For this purpose, the characteristic equation of AVR system is firstly obtained. Secondly, stable K_p - K_i parameter space is obtained by a graphical method stability boundary locus by utilizing this equation. Then, it is determined that the stable K_p - K_i parameter space is the closed area between real root boundary and complex root boundary. Finally, time domain simulations are performed for different PI controller parameters selected in, over and outside of this area. The obtained simulation results prove the accuracy of the method.

Consequently, the stability boundary locus method can also be used as an effective tool to determine the stable PI parameter space for AVR systems. This issue will not only help to determine stability region of PI controller but also help to limit the search space for system optimization problems.

REFERENCES

[1] P. Kundur, *Power System Control and Stability*, vol. Vol. I. McGraw-Hill, 1994.
 [2] H. Saadat, *Power System Analysis*. PSA Publishing LLC, 1994.
 [3] C. W. Taylor, "Power System Voltage Stability," *IEEE Transactions on Power*

- Apparatus and Systems*, vol. PAS-101, no. 10, 1982.
- [4] H. L. Zeynelgil, A. Demirören, and N. S. Şengör, "Load frequency control for power system with reheat steam turbine and governor deadband non-linearity by using neural network controller," *European Transactions on Electrical Power*, vol. 12, no. 3, pp. 179–184, 2002.
- [5] E. Çam, "Application of fuzzy logic for load frequency control of hydroelectrical power plants," *Energy Conversion and Management*, vol. 48, no. 4, pp. 1281–1288, 2007.
- [6] H. Gozde and M. C. Taplamacioglu, "Automatic generation control application with craziness based particle swarm optimization in a thermal power system," *International Journal of Electrical Power and Energy Systems*, vol. 33, no. 1, pp. 8–16, 2011.
- [7] H. Gozde and M. C. Taplamacioglu, "Comparative performance analysis of artificial bee colony algorithm for automatic voltage regulator (AVR) system," *Journal of the Franklin Institute*, vol. 348, no. 8, pp. 1927–1946, 2011.
- [8] İ. Eke, M. C. Taplamacioglu, and K. Y. Lee, "Robust Tuning of Power System Stabilizer by Using Orthogonal Learning Artificial Bee Colony," *IFAC-PapersOnLine*, vol. 48, no. 30, pp. 149–154, 2015.
- [9] M. T. Özdemir, D. Öztürk, I. Eke, V. Çelik, and K. Y. Lee, "Tuning of Optimal Classical and Fractional Order PID Parameters for Automatic Generation Control Based on the Bacterial Swarm Optimization," in *IFAC-PapersOnLine*, 2015, vol. 48, no. 30, pp. 501–506.
- [10] M. F. McGranaghan, D. R. Mueller, and M. J. Samotyj, "Voltage sags in industrial systems," *IEEE Transactions on Industry Applications*, vol. 29, no. 2, pp. 397–403, 1993.
- [11] E. Dembicki and T. Chi, "System analysis in calculation of cantilever retaining walls," *International Journal for Numerical and Analytical Methods in Geomechanics*, vol. 13, no. 6, pp. 599–610, Nov. 1989.
- [12] R. Mohammadi-Milasi, M. J. Yazdanpanah, and P. Jabejdar-Maralani, "A novel adaptive gain-scheduling controller for synchronous generator," in *Proceedings of the 2004 IEEE International Conference on*

- Control Applications*, 2004., 2004, vol. 1, pp. 800–805.
- [13] M. Rezaei Estakhrouieh and A. Gharaveisi, “Optimal iterative learning control design for generator voltage regulation system,” *Turkish Journal of Electrical Engineering & Computer Sciences*, vol. 21, pp. 1909–1919, 2013.
- [14] E. E. Juárez and A. Hernández, “An analytical approach for stochastic assessment of balanced and unbalanced voltage sags in large systems,” *IEEE Transactions on Power Delivery*, vol. 21, no. 3, pp. 1493–1500, 2006.
- [15] M. E. Aboul-Ela, A. A. Sallam, J. D. McCalley, and A. A. Fouad, “Damping controller design for power system oscillations using global signals,” *IEEE Transactions on Power Systems*, vol. 11, no. 2, pp. 767–773, 1996.
- [16] D. İsmail and H. Altaş, “Bulanık Mantık : Bulanıklılık Kavramı,” *Bilesim yayıncılık A.Ş.*, vol. 62, no. 62, pp. 80–85, 1999.
- [17] K. Astrom, “PID controllers: theory, design and tuning,” *Instrument Society of America*. p. 343, 1995.
- [18] U. Eminoglu and S. Ayasun, “Modeling and design optimization of variable-speed wind turbine systems,” *Energies*, vol. 7, no. 1, pp. 402–419, 2014.
- [19] S. Gomes, N. Martins, and C. Portela, “Computing small-signal stability boundaries for large-scale power systems,” *IEEE Transactions on Power Systems*, vol. 18, no. 2, pp. 747–752, 2003.
- [20] N. Tan, I. Kaya, C. Yeroglu, and D. P. Atherton, “Computation of stabilizing PI and PID controllers using the stability boundary locus,” *Energy Conversion and Management*, vol. 47, no. 18–19, pp. 3045–3058, 2006.
- [21] N. Tan and D. P. Atherton, “Design of stabilizing PI and PID controllers,” *International Journal of Systems Science*, vol. 37, no. 8, pp. 543–554, 2006.
- [22] P. Albertos and P. García, “Robust control design for long time-delay systems,” *Journal of Process Control*, vol. 19, no. 10, pp. 1640–1648, 2009.
- [23] N. Tan, “Computation of stabilizing PI and PID controllers for processes with time delay,” *ISA Transactions*, vol. 44, pp. 213–223, 2005.
- [24] F. Koç, V. Çelik, and M. T. Özdemir, “The Effect of Derivative Gain to System Stability in Automatic Voltage Regulator Systems,” in *International Engineering, Science and Education Conference (INESEC)*, 2016, pp. 829–836.
- [25] S. Sonmez and S. Ayasun, “Stability Region in the Parameter Space of PI Controller for a Single-Area Load Frequency Control System With Time Delay,” *IEEE Transactions on Power Systems*, vol. 31, no. 1, pp. 829–830, 2016.
- [26] Z. L. Gaing, “A Particle Swarm Optimization Approach for Optimum Design of PID Controller in AVR System,” *IEEE Transactions on Energy Conversion*, vol. 19, no. 2, pp. 384–391, 2004.
- [27] I. C. Report, “Computer Representation of Excitation Systems,” *IEEE Transactions on Power Apparatus and Systems*, vol. PAS-87, no. 6, pp. 1460–1464, 1968.
- [28] PES, *IEEE Recommended Practice for Excitation System Models for Power System Stability Studies*, vol. 2005, no. April. 2006.
- [29] S. E. Hamamci, “An algorithm for stabilization of fractional-order time delay systems using fractional-order PID controllers,” *IEEE Transactions on Automatic Control*, vol. 52, no. 10, pp. 1964–1969, 2007.